

Studies on the Effect of the Substrate on the Electrocatalytic Performance of Electrodeposited NiFe Hydroxides for Oxygen Evolution Reaction

Hansheng Wei², Jie Liu^{1,*}, Yida Deng¹, Wenbin Hu¹ and Cheng Zhong^{1,*}

¹ School of Materials Science and Engineering, Tianjin University, Tianjin 300072, China

² Fujian Jianou First High School, Fujian 353100, China

*E-mails: jieliu0109@tju.edu.cn; cheng.zhong@tju.edu.cn

Received: 4 January 2019 / Accepted: 28 February 2019 / Published: 10 April 2019

As one of the most promising candidates for the oxygen evolution reaction (OER), NiFe hydroxides have attracted tremendous attention due to their earth abundance, cost-effectiveness, and relatively high catalytic activity. In this work, to investigate the effect of the underlying substrate on the electrocatalytic activity of NiFe hydroxides for the OER, NiFe hydroxides were prepared on various substrates including Au, Cu, C, ITO, and Ti via an electrodeposition technique. The whole preparation process is extremely clean since it avoids the introduction of any surfactants, binders, reducers or capping agents, ensuring the clean surface of NiFe hydroxides and thus allowing a true comparison of the effect of the substrate composition on the electrocatalytic performance of NiFe hydroxides. The surface morphology and chemical element distribution of the electrodes were studied by a scanning electron microscope and energy dispersive X-ray analysis, and the chemical composition was characterized by X-ray photoelectron spectroscopy. The NiFe hydroxides electrodeposited on various substrates exhibit similar thin film surface morphologies and are grown horizontally on the surface of the substrate, possessing some small wrinkles approximately vertically aligned to the surface. Among the NiFe hydroxides formed on the various substrates, the NiFe hydroxides on the Au substrate exhibit the most remarkable enhancement in electrocatalytic activity towards the OER, and the current density reaches 149 mA cm^{-2} at 0.8 V (vs. saturated calomel electrode). The catalytic current density shows no evident decay after an accelerated durability test of 10000 s. This work provides a systematic study on the influence of the substrate composition on the electrocatalytic activity of electrodeposited NiFe hydroxides and demonstrates new ways to develop high-performance catalysts.

Keywords: NiFe hydroxides; electrodeposition; substrate composition; oxygen evolution reaction

1. INTRODUCTION

Facing deteriorating energy and environmental issues, the search for sustainable and clean energy sources to replace fossil fuels has become one of the most important tasks of the 21st century

[1-5]. Water-splitting reactions have attracted numerous interests due to their unique role in clean energy conversion techniques, especially the production of hydrogen and oxygen [6-10]. However, the sluggish kinetics of the oxygen evolution reaction (OER) significantly restrict the practical application of electrochemical water splitting, and thus, it is of great importance to develop efficient electrocatalysts [11-13]. To date, noble metal-based materials, such as Ir- and Ru-containing compounds, have been widely used for their high OER efficiency, but their scarcity and high cost render large-scale commercialization infeasible [14-16]. To address this issue, tremendous attention has been devoted to transition-metal (Mn, Fe, Co, and Ni) oxide/hydroxide catalysts, whose advantages mainly lie in their earth abundance, cost-effectiveness, and high catalytic activity [17, 18]. In particular, NiFe hydroxides are viewed as a representative catalyst with a high OER activity, which could effectively catalyze ongoing electrochemical reactions [19-21].

To further improve the electrocatalytic activity of NiFe hydroxides, extensive efforts have been devoted to the preparation of NiFe hydroxides with controllable morphology and composition [22-28]. However, research into the effect of the underlying substrate on the performance of electrocatalysts has been rather limited. Previous studies have found that the catalyst substrate plays an important role in developing highly active catalysts, in which the substrate composition significantly influences the overall catalytic performance [29, 30]. For instance, Wu et al. [31, 32] found that a Pt@TiO₂ catalyst possessed a much higher photocatalytic activity than that of pristine TiO₂, which also surpassed that of Au@TiO₂. Previous work from our group described a Pt monolayer supported on an Au nanoparticle that exhibited a specific activity towards ammonia electro-oxidation approximately 8.3-times higher than that of the monolayers supported on Ru and Pd nanoparticles. This improvement could be attributed to the substrate-induced tensile strain in the Pt monolayer resulting from the lattice mismatch between the Pt monolayer and Au nanoparticle support [33]. Despite evidence that the substrate composition exerts such a considerable influence on the overall electrocatalytic performance, few efforts have been devoted to the systematic research on the effect of substrate composition on the OER performance of NiFe hydroxides.

In this work, we developed a facile and extremely clean electrochemical method to directly synthesize NiFe hydroxides on the surface of various substrates, including Au, Cu, C, ITO and Ti, and explored the effect of the substrate composition on the OER catalytic performance of formed NiFe hydroxides. The electrodeposition technique provides an ideal way to conduct the overall research because it avoids the use of surfactants, conductive additives and binding agents during the electrode preparation process, ensuring a clean surface of the electrocatalyst; and thus allowing a true comparison of the OER electrocatalytic performances of NiFe hydroxides formed on substrates of different compositions. The surface morphology and chemical element distribution of the as-prepared electrodes were characterized by a scanning electron microscope (SEM) equipped with energy dispersive X-ray analysis (EDX), and the chemical composition was characterized by X-ray photoelectron spectroscopy (XPS). Among the NiFe hydroxides formed on various substrates, NiFe hydroxides/Au exhibits the most remarkable enhancement in electrocatalytic activity towards the OER, with a current density reaching 149 mA cm⁻² at 0.8 V. The catalytic current density shows no apparent decay after an accelerated durability test (ADT) of 10000 s.

2. EXPERIMENTAL

2.1 Reagents

The reagents, such as $\text{Ni}(\text{NO}_3)_2$, $\text{Fe}(\text{NO}_3)_3$ and KOH , were purchased from Macklin Biochemical Co., Ltd. All chemicals were used as received without further purification. All reagents were of analytical grade and were used directly without further purification. All the aqueous solutions used in the present work were prepared with ultrapure water (Milli-Q Millipore, $> 18.2 \text{ M}\Omega \text{ cm}$).

2.2 Electrodeposition of NiFe hydroxides

NiFe hydroxides were prepared via an electrodeposition technique with a three-electrode system, in which Au foil ($1 \times 1 \text{ cm}^2$), Cu foil ($1 \times 1 \text{ cm}^2$), carbon film (C, $1 \times 1 \text{ cm}^2$), indium tin oxide (ITO, $1 \times 1 \text{ cm}^2$), or Ti foil ($1 \times 1 \text{ cm}^2$) was used as the working electrode, a platinum sheet ($1 \times 1 \text{ cm}^2$) was used as the counter electrode, and a saturated calomel electrode (SCE) was used as the reference electrode. The aqueous electrolyte solution contained 3 mM $\text{Ni}(\text{NO}_3)_2$ and 3 mM $\text{Fe}(\text{NO}_3)_3$. The electrodeposition was performed with an electrochemical workstation (CHI660D, USA). Some preliminary experiments had been performed to determine the optimal electrodeposition potentials and times, and the following conditions were used to prepare NiFe hydroxides on different substrates. The electrodeposition potential was -1 V . For the preparation of NiFe/Au and NiFe/Cu, the electrodeposition time was 60 s, and the electrodeposition time was 120 s for NiFe/C, NiFe/ITO and NiFe/Ti. After the electrodeposition, the samples were washed with deionized water and dried in an air atmosphere.

2.3 Materials Characterization

The surface morphology of the samples was characterized by a scanning electron microscope (SEM, Hitachi S-4800, Hitachi, Japan), and the corresponding elemental mapping was obtained by the energy-dispersive X-ray spectrometer (EDX) equipped with the SEM. The chemical composition of the prepared samples was investigated by X-ray photoelectron spectroscopy (XPS, Escalab 250XI, ThermoFisher Scientific, USA).

2.4 Electrochemical Measurements

A three-electrode system was used in the electrochemical tests. The as-prepared electrode was used as the working electrode, and a platinum sheet ($1 \times 1 \text{ cm}^2$) and a calomel electrode (SCE) served as the counter electrode and the reference electrode, respectively. The aqueous electrolyte solution contained 1 M KOH . The linear sweep voltammetry (LSV) measurements were performed between 0 V and 0.8 V, and the scan rate was 5 mV s^{-1} . In the electrochemical impedance spectra (EIS) measurement, the applied voltage was 0.6 V. For the long-term stability testing, the applied voltage was 0.6 V, and the test time was 10000 s.

3. RESULTS AND DISCUSSION

Fig. 1 shows the SEM images of electrodeposited NiFe hydroxides on different substrates including Au, Cu, C, Ti, and ITO. Due to the different natures of these five substrates, it is difficult to obtain NiFe hydroxides with exactly the same surface morphology on various substrates. As mentioned in the experimental section, preliminary work tried various electrodeposition parameters, including deposition potential and time, and finally found the optimal conditions to obtain NiFe hydroxides with similar surface morphologies.

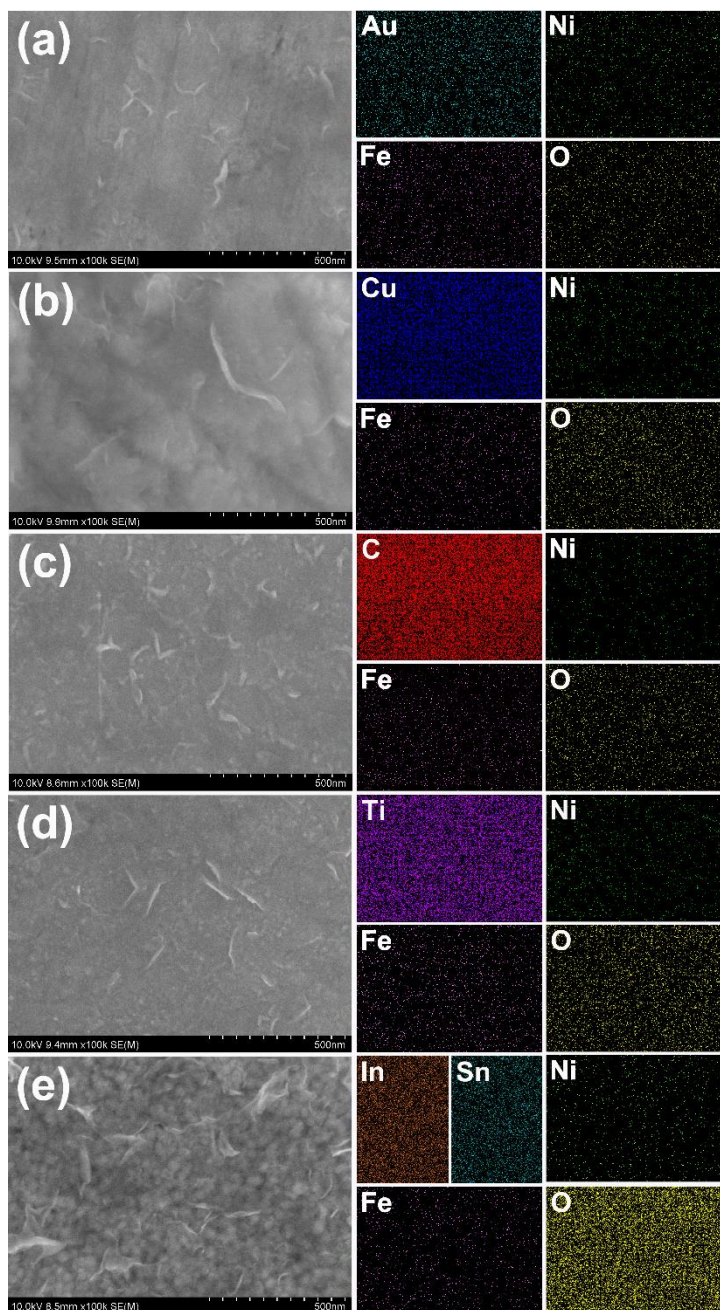


Figure 1. SEM images and EDX maps of electrodeposited NiFe hydroxides on different substrates including (a) Au, (b) Cu, (c) C, (d) Ti, and (e) ITO.

This result is important for the following tests since we can minimize the morphological effect on the electrocatalytic performance and focus on the effect of the substrate on the electrocatalytic performance of electrodeposited NiFe hydroxides. Although NiFe hydroxides were electrodeposited on different substrates, they exhibit similar surface morphologies and are horizontally and uniformly grown on the surface. The reduction reaction of NO_3^- anions at the electrode surface during the electrodeposition process generates local hydroxide ions that react with Ni^{2+} and Fe^{3+} ions to form NiFe hydroxide films on the substrate surface [34, 35]. Additionally, some small and approximately vertically aligned wrinkles can be observed on the surface, which have also been reported in previous studies on electrodeposited NiFe hydroxides [36, 37]. Such wrinkles are a typical characteristic of NiFe hydroxides [38], and their formation is associated with the presence of flexible and ultrathin layered double hydroxides [39]. In addition, EDX elemental mapping was performed to investigate the surface chemistry of the as-prepared electrodes. As shown in Fig. 1, Ni, Fe, and O elements are found for all the as-prepared samples, demonstrating the successful synthesis of NiFe hydroxides on the different substrates. Furthermore, the Ni, Fe and O elements are uniformly distributed on the different substrate surfaces, indicating that the various substrates are uniformly covered with NiFe hydroxides. The combined SEM images and EDX elemental mapping results confirm that the NiFe hydroxides are horizontally grown on the surface of different substrates. The horizontal growth of the NiFe hydroxide film on the surface of a substrate results in a large contact area between the thin NiFe hydroxide film and the substrate, ensuring the good electrical conductivity. Additionally, the signals from the substrates (i.e., Au, Cu, C, In, Sn, and Ti) are also collected due to the relatively large information depth (several μm) of EDX analysis.

The chemical states of the as-prepared samples were investigated by X-ray photoelectron spectroscopy (XPS). As shown in the XPS survey spectra of Fig. 2a, Ni, Fe, and O are obtained, which are consistent with the EDX mapping results (Fig. 1). The peaks at approximately 856.0 eV and 874.0 eV in the high-resolution spectra of Ni 2p are ascribed to Ni 2p_{3/2} and Ni 2p_{1/2}, respectively, and the satellite peaks of Ni are also observed at approximately 862.0 eV and 880.0 eV, indicating the existence of Ni in the Ni^{2+} state [34, 35] (Fig. 2b). Fe 2p_{3/2} and Fe 2p_{1/2} at approximately 712.0 eV and 726.0 eV, respectively, reveal that Fe^{3+} is the oxidation state of the Fe element in the NiFe hydroxides [34, 35] (Fig. 2c). The O 1s high-resolution spectra show a peak at the binding energy of 532.0 eV, which corresponds to the hydroxyl group in NiFe hydroxides (Fig. 2d). Clearly, similar XPS spectra are observed for the NiFe hydroxides electrodeposited on Au, Cu, C, Ti and ITO substrates (Fig. 2). This result again suggests the successful formation of NiFe hydroxides with the same chemical composition on different substrates prepared by the electrodeposition method.

To evaluate their electrocatalytic properties for the OER, the NiFe hydroxides on different substrates were tested in a 1.0 M KOH alkaline electrolyte by LSV using a three-electrode system. As shown in Fig. 3a, the NiFe hydroxides on different substrates exhibit different onset potentials, overpotentials, and OER current densities, although they have similar surface morphologies and the same chemical composition. This result clearly suggests that the underlying substrate demonstrates a strong influence on the electrocatalytic performance of NiFe hydroxides towards the OER.

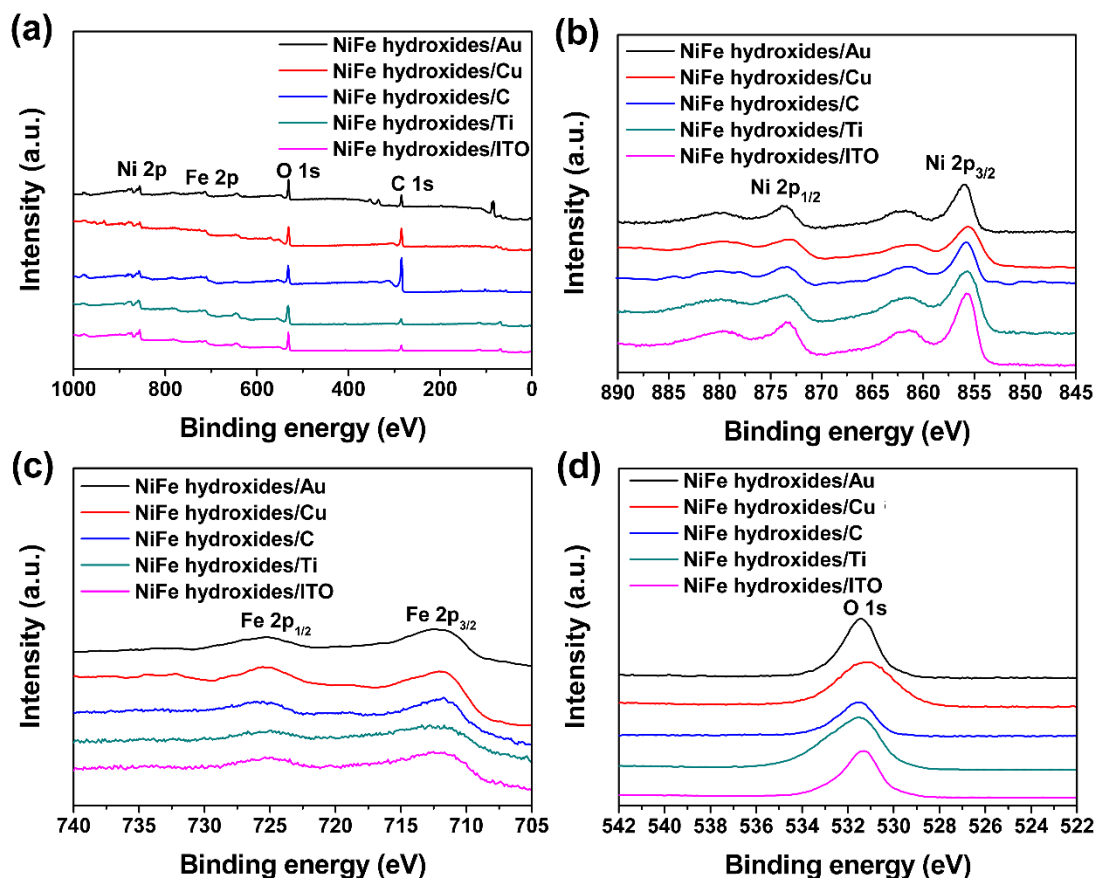


Figure 2. a) XPS survey spectra and the expanded XPS spectra for the b) Ni 2p, c) Fe 2p and d) O 1s of NiFe hydroxides on different substrates.

The NiFe hydroxides electrodeposited on the Au substrate present the lowest onset potential (defined as the potential where the current density reaches 2 mA cm^{-2}) of 0.44 V (vs. SCE), which outperforms that of NiFe hydroxides/ITO (0.52 V (vs. SCE)) and NiFe hydroxides/Ti (0.67 V (vs. SCE)). Moreover, the NiFe hydroxides electrodeposited on the Au substrate exhibit the lowest overpotential among all the investigated electrodes. In particular, the NiFe hydroxides/Au shows the largest current density of 149 mA cm^{-2} at 0.8 V (vs. SCE), which is 1.3–1.8-times higher than that of the NiFe hydroxides/Cu and the NiFe hydroxides/C and is more than a magnitude larger than that of NiFe hydroxides/ITO and NiFe hydroxides/Ti. Fig. 3b shows the corresponding Tafel plots of the NiFe hydroxides on different substrates. The fitted Tafel slope value of NiFe hydroxides/Au (65 mV dec^{-1}) is substantially lower than that of the other electrodes (e.g., 115 mV dec^{-1} for NiFe hydroxides/Cu and 110 mV dec^{-1} for NiFe hydroxides/C), indicating the considerably more favorable OER kinetics over the surface of NiFe hydroxides/Au. Therefore, the substrate of the electrocatalyst plays a significant role in the OER electrocatalytic activity, and the Au substrate contributes to the most remarkable OER performance enhancement for NiFe hydroxides.

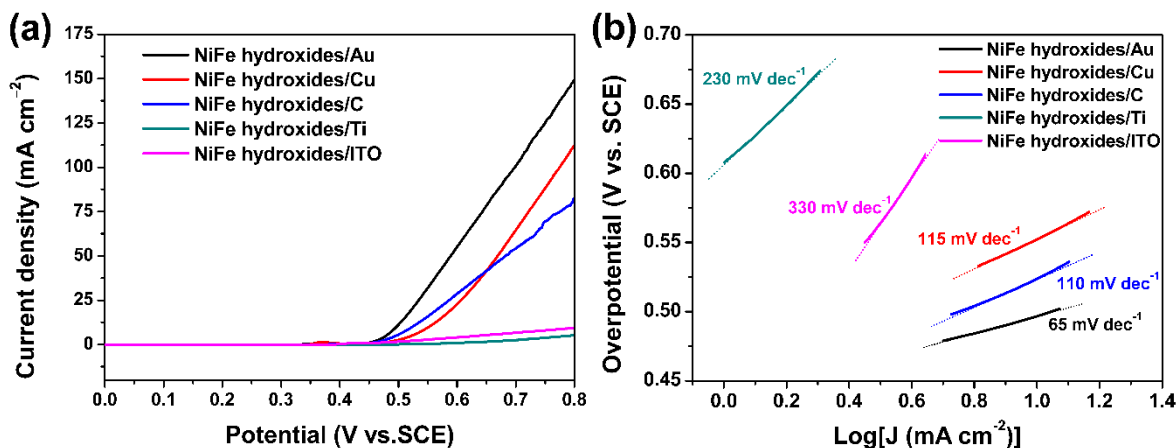


Figure 3. (a) OER polarization curves and (b) corresponding Tafel plots of the NiFe hydroxides on different substrates tested in a 1.0 M KOH solution at 50 mV s⁻¹.

To further investigate the OER performance of the NiFe hydroxides on different substrates, electrochemical impedance spectroscopy (EIS) experiments were performed to explore the charge-transfer properties during the OER process. The charge transfer resistance (R_{ct}) is directly related to the diameter of the semicircle. A smaller charge transfer resistance suggests faster OER catalytic kinetics [40]. As shown in Fig. 4, the R_{ct} of the tested samples follows the order NiFe hydroxides/Au < NiFe/Cu < NiFe/C < NiFe/ITO < NiFe/Ti, which is consistent with the trend of the LSV results. Obviously, NiFe/Au has the lowest R_{ct} of 1.1 Ω cm² (Fig. 4b), suggesting the fastest charge transport and electrocatalytic kinetics among all these electrodes. A possible explanation is that the synergistic interaction between the as-deposited NiFe hydroxides and the Au substrate lowers the charge transfer resistance at the interface between the electrocatalyst and the substrate, accelerating the electrocatalytic kinetics [29, 41, 42]. Furthermore, the direct deposition of NiFe hydroxides on the Au substrate ensures close adhesion between NiFe hydroxides and the Au substrate, resulting in efficient electron transport during catalysis of the OER [42].

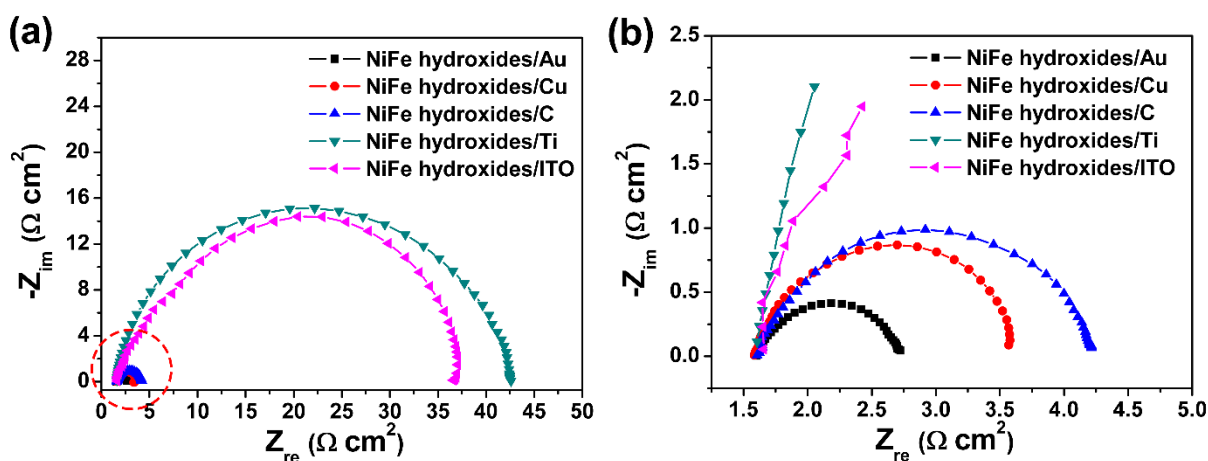


Figure 4. (a) EIS plots of the NiFe hydroxides on the different substrates tested in a 1.0 M KOH solution at 0.6 V (vs. SCE) and (b) the enlarged plots of the EIS marked in the red circle.

Since the NiFe hydroxides/Au electrode exhibits the highest electrocatalytic activity towards the OER, the long-term stability of this sample was further investigated. As shown in Fig. 5, the electrochemical stability of NiFe hydroxides/Au was investigated by the chronopotentiometry technique at 0.6 V (vs. SCE), during which the OER current density reaches 52 mA cm^{-2} . No noticeable decay in the current density during 10000 s is observed, demonstrating the excellent long-term electrocatalytic stability of NiFe hydroxides/Au towards the OER. The high electrocatalytic stability of NiFe hydroxides/Au towards the OER is mainly attributed to three factors: 1) Au is a chemically inert metal and possesses good chemical and electrochemical stability in alkaline solutions, providing a highly stable substrate to support the NiFe hydroxides during the OER process. 2) The intimate adhesion between the NiFe hydroxides and the Au substrate guarantees stable electrical transport between the electrocatalyst and the substrate. 3) Since the NiFe hydroxide thin film is horizontally and uniformly grown on the surface of the Au substrate, the Au substrate can effectively inhibit the agglomeration of the NiFe hydroxide film during the OER, improving the electrocatalytic stability of NiFe hydroxides/Au.

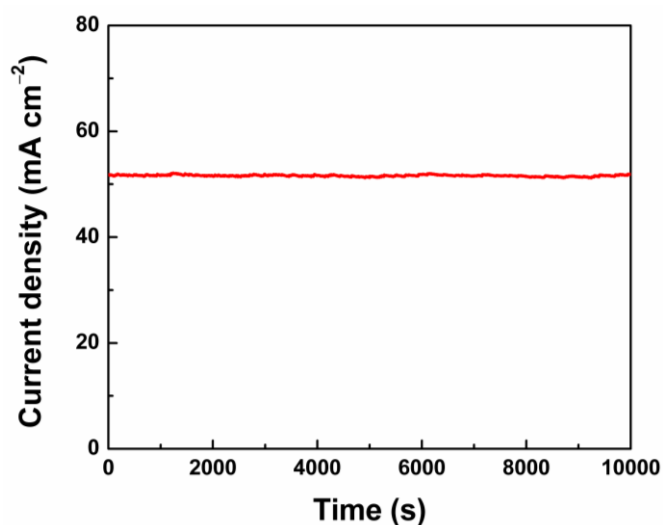


Figure 5. Chronoamperometry curve obtained with the NiFe hydroxides/Au electrode in 1.0 M KOH with a constant potential of 0.6 V (vs. SCE).

To further explain the high electrocatalytic performance of the NiFe hydroxides/Au catalyst for the OER, an SEM image of the NiFe hydroxides/Au catalyst after the ADT is provided in Fig. 6. Compared to the surface morphology of the NiFe hydroxides/Au electrode before the ADT (Fig. 1a), the surface morphology of the NiFe hydroxides/Au catalyst after the ADT is slightly rough due to the formation of some wrinkles, possibly caused by the surface tension of evolving oxygen bubbles. However, the thin NiFe hydroxide film on the surface of the Au substrate preserves a surface morphology similar to that exhibited before the ADT (Fig. 1a), and no evident detachment or dissolution of NiFe hydroxides from the Au substrate is observed, revealing the good electrochemical stability of the NiFe hydroxides on the Au substrate. This behavior explains well the high electrocatalytic stability of NiFe hydroxides/Au towards the OER (Fig. 5) and further supports the view that the Au substrate can effectively inhibit the agglomeration of the NiFe hydroxide film.

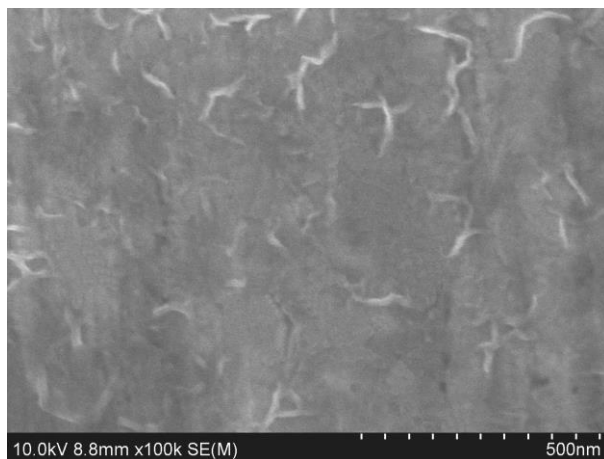


Figure 6. SEM image of the NiFe hydroxides/Au electrode after the ADT.

In addition, XPS of the NiFe hydroxides formed on the Au substrate after the ADT was conducted (Fig. 7a). Compared to the XPS results for freshly prepared NiFe hydroxides/Au (Fig. 2), no distinct absence of Ni, Fe or O peaks are observed after the ADT. This result indicates that the NiFe hydroxides do not significantly dissolve or fall off from the Au substrate, which is consistent with the SEM result of NiFe hydroxides/Au after the ADT (Fig. 6). The high-resolution XPS spectra of Ni and Fe elements (Figs. 7b, and c) show that Ni 2p, Fe 2p and O 1s still exhibit their characteristic peaks (Figs. 2b–d) [43, 44], suggesting that after the ADT, the chemical states of Ni, Fe and O elements in the NiFe hydroxides remain unchanged. The above results suggest that the NiFe hydroxides electrodeposited on the Au substrate possess a high electrochemical stability during the OER process. Among the as-prepared NiFe hydroxides on various substrates, the NiFe hydroxides formed on the Au substrate present the highest electrocatalytic activity towards the OER, although the film has a similar surface morphology and the same chemical state compared to NiFe hydroxides grown on other substrates. This observation clearly demonstrates that the underlying Au substrate plays a vital role in the enhancement of the activity of the electrocatalyst towards the OER. The electrical conductivities of the underlying Au ($4.3 \times 10^5 \text{ S cm}^{-1}$) and Cu ($5.8 \times 10^5 \text{ S cm}^{-1}$) substrates at room temperature are much larger than those of Ti ($2.4 \times 10^4 \text{ S cm}^{-1}$) and ITO ($2.0 \times 10^3 \text{ S cm}^{-1}$), and far larger than that of the carbon substrate (12.5 S cm^{-1}). It has been generally accepted that a substrate with a high electrical conductivity is beneficial to improve the electrocatalytic activity of catalysts. This relationship is also the case in the present work. For example, the electrocatalytic activities of NiFe hydroxides/Cu and NiFe hydroxides/Au are substantially higher than those of NiFe hydroxides/Ti and NiFe hydroxides/ITO. However, it is interesting to note that, although the electrical conductivity of the Cu substrate is higher than that of the Au substrate, the electrocatalytic activity of NiFe hydroxides/Au is higher than that of NiFe hydroxides/Cu. This suggests that the electrical conductivity of the substrate is not the only factor determining the electrocatalytic activity of the NiFe hydroxides. The electronegativity of the underlying substrate is also expected to affect the electrocatalytic activity of the NiFe hydroxides. Compared to Cu, Au is more electronegative and thus, to a greater extent, promotes the oxidation of Ni into an active species with a higher valence state. A similar phenomenon has also been reported by Sayeed et al. [43] for a $\text{Co}(\text{OH})_2$ catalyst on a Au substrate. Therefore, both

the high electrical conductivity of the Au substrate and the strong synergism between the NiFe hydroxides and Au substrate contribute to the highest electrocatalytic activity of NiFe hydroxides grown on the Au substrate.

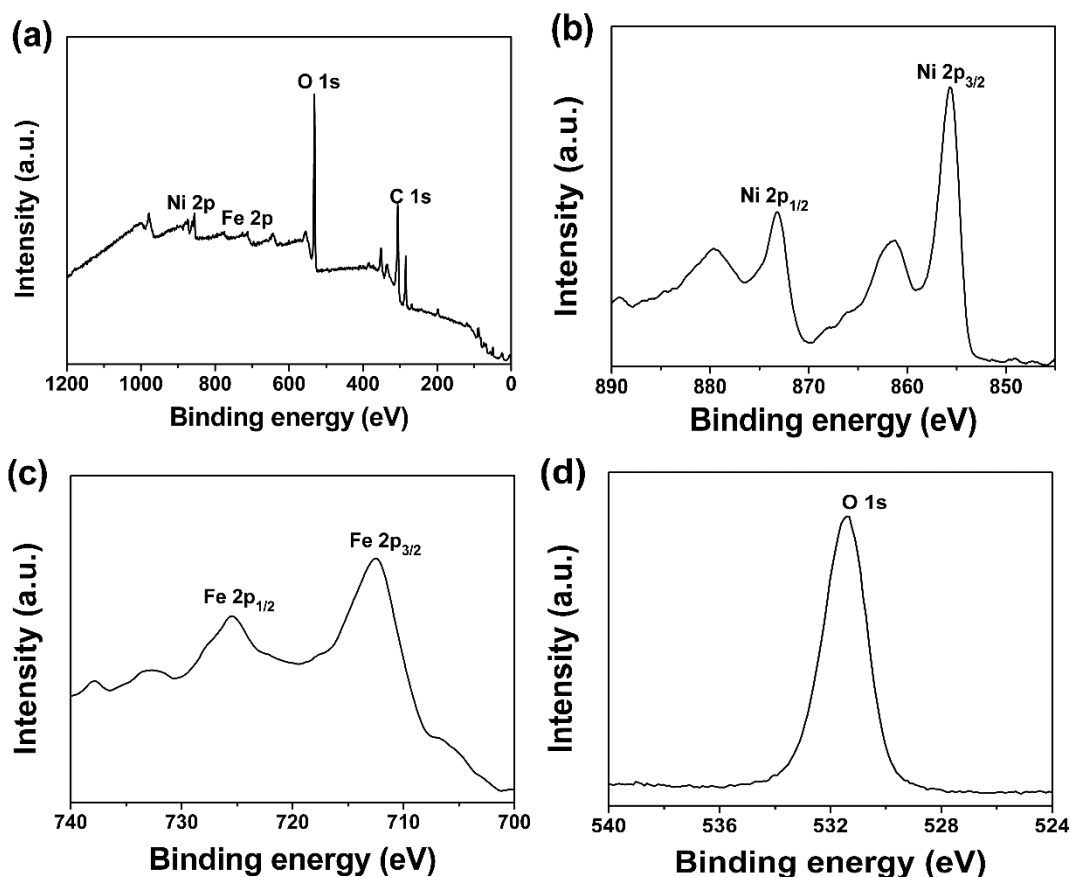


Figure 7. a) XPS survey spectrum and high-resolution XPS spectra for the b) Ni 2p, c) Fe 2p and d) O 1s of the NiFe hydroxides on the Au substrate after the ADT.

4. CONCLUSIONS

In the present work, the effect of the substrate composition on the electrocatalytic activity of NiFe hydroxides was investigated. NiFe hydroxides were directly formed on the surfaces of a series of substrates including Au, Cu, C, ITO, and Ti by a clean and facile electrodeposition method. The electrodeposited NiFe hydroxide thin films exhibit similar surface morphologies and are horizontally and uniformly grown on the surfaces of various substrates. Among the NiFe hydroxides formed on the various substrates, the NiFe hydroxides formed on the Au substrate exhibit the highest electrocatalytic activity towards the OER, and the current density reaches 149 mA cm^{-2} at 0.8 V (vs. SCE); this value is 1.3~1.8 times higher than that obtained on the Cu and C substrates and is more than a magnitude larger than that obtained on the ITO and Ti substrates. The EIS results reveal much lower charge transfer resistance for the OER of the NiFe hydroxides on the Au substrate compared to that of the NiFe hydroxides formed on the other substrates. Moreover, no apparent decay in the electrocatalytic

activity of NiFe hydroxides/Au is observed after the ADT, revealing the high electrochemical stability of the NiFe hydroxides. The enhanced electrocatalytic activity of the NiFe hydroxides formed on the Au substrate is attributed to not only the high electrical conductivity of the substrate but also the synergistic effect between the NiFe hydroxides and Au substrate.

ACKNOWLEDGMENTS

This work was supported by the National Science Foundation for Excellent Young Scholar (No. 51722403), National Natural Science Foundation of China (Nos. 51771134 and 51801134), National Natural Science Foundation of China and Guangdong Province (No. U1601216), Tianjin Natural Science Foundation (Nos. 18JCJQJC46500 and 16JCYBJC17600), and the National Youth Talent Support Program. The authors would like to thank Jianfeng Wang from Shiyanjia Lab (www.shiyanjia.com) for the XPS analysis.

CONFLICTS OF INTEREST

The authors declare no conflict of interest.

References

1. J. Liu, J. Xu, Y. Chen, W. Sun, X. Zhou, J. Ke, *Int. J. Electrochem. Sci.*, 14 (2019) 359.
2. Y. Wang, S. Liu, N. Zhang, X. Qiao, Z. Zhou, *Int. J. Electrochem. Sci.*, 14 (2019) 618.
3. S. Wang, W. Li, H. Qin, L. Liu, Y. Chen, D. Xiang, *Int. J. Electrochem. Sci.*, 14 (2019) 957.
4. X. Chen, B. Liu, C. Zhong, Z. Liu, J. Liu, L. Ma, Y. Deng, X. Han, T. Wu, W. Hu, J. Lu, *Adv. Energy Mater.*, 7 (2017) 1700779.
5. X. Fan, J. Liu, Z. Song, X. Han, Y. Deng, C. Zhong, W. Hu, *Nano Energy*, 56 (2019) 454.
6. X. Han, X. Wu, Y. Deng, J. Liu, J. Lu, C. Zhong, W. Hu, *Adv. Energy Mater.*, 8 (2018) 1800935.
7. W. Lu, P. Yuan, F. Wei, K. Cheng, W. Li, Y. Zhou, W. Zheng, G. Zhang, *Int. J. Electrochem. Sci.*, 13 (2018) 3235.
8. F. Zhao, T. Sun, N. Xia, *Int. J. Electrochem. Sci.*, 13 (2018) 4601.
9. J. Liu, J. Wang, B. Zhang, Y. Ruan, L. Lv, X. Ji, K. Xu, L. Miao, J. Jiang, *ACS Appl. Mater. Interfaces*, 9 (2017) 15364.
10. Z. Song, X. Han, Y. Deng, N. Zhao, W. Hu, C. Zhong, *ACS Appl. Mater. Interfaces*, 9 (2017) 22694.
11. B. Liu, S. Qu, Y. Kou, Z. Liu, X. Chen, Y. Wu, X. Han, Y. Deng, W. Hu, C. Zhong, *ACS Appl. Mater. Interfaces*, 10 (2018) 30433.
12. S. Qu, Z. Song, J. Liu, Y. Li, Y. Kou, C. Ma, X. Han, Y. Deng, N. Zhao, W. Hu, C. Zhong, *Nano Energy*, 39 (2017) 101.
13. Z. Wu, Z. Zou, J. Huang, F. Gao, *ACS Appl. Mater. Interfaces*, 10 (2018) 26283.
14. H. Xu, B. Wang, C. Shan, P. Xi, W. Liu, Y. Tang, *ACS Appl. Mater. Interfaces*, 10 (2018) 6336.
15. L. Yang, L. Xie, R. Ge, R. Kong, Z. Liu, G. Du, A.M. Asiri, Y. Yao, Y. Luo, *ACS Appl. Mater. Interfaces*, 9 (2017) 19502.
16. K. Yan, T. Lafleur, J. Chai, C. Jarvis, *Electrochem. Commun.*, 62 (2016) 24.
17. X. Chen, C. Zhong, B. Liu, Z. Liu, X. Bi, N. Zhao, X. Han, Y. Deng, J. Lu, W. Hu, *Small*, 14 (2018) 1702987.
18. Y. Li, C. Zhong, J. Liu, X. Zeng, S. Qu, X. Han, Y. Deng, W. Hu, J. Lu, *Adv. Mater.*, 30 (2018) 1703657.
19. O. Diaz-Morales, I. Ledezma-Yanez, M.T.M. Koper, F. Calle-Vallejo, *ACS Catalysis*, 5 (2015) 5380.
20. X. Su, Q. Sun, J. Bai, Z. Wang, C. Zhao, *Electrochim. Acta*, 260 (2018) 477.

21. Y. Li, C. Zhao, *ACS Catalysis*, 7 (2017) 2535.
22. H. Liang, A.N. Gandi, C. Xia, M.N. Hedhili, D.H. Anjum, U. Schwingenschlöggl, H.N. Alshareef, *ACS Energy Letters*, 2 (2017) 1035.
23. K. Zhang, W. Wang, L. Kuai, B. Geng, *Electrochim. Acta*, 225 (2017) 303.
24. T. Wang, G. Nam, Y. Jin, X. Wang, P. Ren, M.G. Kim, J. Liang, X. Wen, H. Jang, J. Han, Y. Huang, Q. Li, J. Cho, *Adv. Mater.*, 30 (2018) 1800757.
25. H. Zhang, H. Li, B. Akram, X. Wang, *Nano Research*, (2019).
26. Q. Liu, H. Wang, X. Wang, R. Tong, X. Zhou, X. Peng, H. Wang, H. Tao, Z. Zhang, *Int. J. Hydrogen Energy*, 42 (2017) 5560.
27. B. Wang, C. Tang, H.-F. Wang, B.-Q. Li, X. Cui, Q. Zhang, *Small Methods*, 2 (2018) 1800055.
28. Z. Lu, W. Xu, W. Zhu, Q. Yang, X. Lei, J. Liu, Y. Li, X. Sun, X. Duan, *Chem. Commun.*, 50 (2014) 6479.
29. J. Zhang, J. Liu, L. Xi, Y. Yu, N. Chen, S. Sun, W. Wang, K.M. Lange, B. Zhang, *J. Am. Chem. Soc.*, 140 (2018) 3876.
30. A.L. Strickler, M. Escudero-Escribano, T.F. Jaramillo, *Nano Lett.*, 17 (2017) 6040.
31. X.-F. Wu, Y.-F. Chen, J.-M. Yoon, Y.-T. Yu, *Mater. Lett.*, 64 (2010) 2208.
32. X.-F. Wu, H.-Y. Song, J.-M. Yoon, Y.-T. Yu, Y.-F. Chen, *Langmuir*, 25 (2009) 6438.
33. J. Liu, B. Liu, Y. Wu, X. Chen, J. Zhang, Y. Deng, W. Hu, C. Zhong, *Catalysts*, 9 (2018) 4.
34. M. Zhang, Z. Wei, T. Wang, S. Muhammad, J. Zhou, J. Liu, J. Zhu, J. Hu, *Electrochim. Acta*, 296 (2019) 190.
35. X. Lu, C. Zhao, *Nat. Commun.*, 6 (2015) 6616.
36. A.S. Batchellor, S.W. Boettcher, *ACS Catalysis*, 5 (2015) 6680.
37. W. Zhang, Y. Wu, J. Qi, M. Chen, R. Cao, *Adv. Energy Mater.*, 7 (2017) 1602547.
38. F. Dionigi, P. Strasser, *Adv. Energy Mater.*, 6 (2016) 1600621.
39. K. Zhou, R. Gao, X. Qian, *J. Hazard. Mater.*, 338 (2017) 343.
40. Y. Li, J. Fu, C. Zhong, T. Wu, Z. Chen, W. Hu, K. Amine, J. Lu, *Adv. Energy Mater.*, 9 (2019) 1802605.
41. G. Chen, T. Ma, Z. Liu, N. Li, Y. Su, K. Davey, S. Qiao, *Adv. Funct. Mater.*, 26 (2016) 3314.
42. J. Ruan, W. Zhao, L. Wu, X. Li, X. Zheng, Q. Ye, X. Xu, F. Wang, *Appl. Surf. Sci.*, 396 (2017) 1146.
43. M.A. Sayeed, T. Herd, A.P. O'Mullane, *J. Mater. Chem. A*, 4 (2016) 991.
44. H.B. Li, M.H. Yu, X.H. Lu, P. Liu, Y. Liang, J. Xiao, Y.X. Tong, G.W. Yang, *ACS Appl. Mater. Interfaces*, 6 (2014) 745.